Journal Name

Dynamic Article Links ►

Cite this: DOI: 10.1039/c0xx00000x

www.rsc.org/xxxxxx

ARTICLE TYPE

Instant inactivation and rapid decomposition of *Escherichia coli* using high efficiency TiO_2 nanotube array photoelectrode

Xiaolu Liu,[a] Yanhe Han,*[a,b] Guiying Li,[c] Haimin Zhang*[a] and Huijun Zhao[a]

Received (in XXX, XXX) Xth XXXXXXXXX 200X, Accepted Xth XXXXXXXXX 200X

DOI: 10.1039/b000000x

Highly ordered TiO_2 nanotube (TNT) array film fabricated by anodisation was used as photoelectrode in a thin-layer photoelectrochemical flow reactor, exhibiting excellent capability of instant inactivation and rapid decomposition of *Escherichia coli* (*E. coli*). With photoelectrocatalytic (PEC) treatment, 100% inactivation of *E. coli* (1.0×10^7 CFU/mL) can be achieved within 97 s using TNT, which was almost 2.2 times faster than using TiO_2 nanoparticle (TNP) photoelectrode with a similar film thickness. The high efficiency TNT photoelectrode combining with the thin-layer photoelectrochemical flow reactor would be promising for scaling up application to effectively remove waterborne pathogens.

1 Introduction

Highly ordered TiO_2 nanotubes (TNTs) fabricated by anodisation have shown great potential in photocatalysis, photovoltaics, photoelectrocatalysis, biomedicine and sensing.[1-5] It has been reported that in a TiO_2 nanotube film, the recombination rate of photoelectrons and holes is almost 10 times slower than that in a TiO_2 nanoparticle film.[6, 7] In this respect, our group has developed a photoelectrochemical approach to quantitatively characterise the photocatalytic resistance of a photocatalyst film.[8-11] Using this method, the calculated photocatalytic resistances of TiO_2 nanotube and nanoparticle films are 42 Ω and 245 Ω, respectively.[8, 9] Obviously, the highly ordered TiO_2 nanotube array film possesses lower photocatalytic resistance and higher photocatalytic efficiency, which can be ascribed to the unique one-dimensional nanotubular structure providing superior electron transport pathway, thus effectively compressing the recombination of the photogenerated electron/hole pairs.[9]

Due to the excellent photocatalytic activity, TiO_2 photocatalyst has been widely utilised not only to decompose organic pollutants but also to inactivate microorganisms.[12, 13] Although the killing mechanisms remain controversial to date, it has been generally agreed that the bactericidal effect of TiO_2 photocatalyst can be ascribed to the superior oxidative power of the active oxygen species (AOSs) such as $^{\cdot}OH$, $H_2O^{\cdot}$, $O_2^{\cdot-}$, $HOO^{\cdot}$ and H_2O_2 under irradiation.[14] However, in a traditionally photocatalytic process (particle suspension system), high recombination of photogenerated electrons and holes, and short lifetime of the AOSs have been the biggest limitation of application.[15] A solution can be achieved by using photoelectrocatalytic technique, by which the photooxidation and reduction half-reaction can be effectively separated, thus inhibiting the recombination of photogenerated electrons and holes, and improving the lifetime of photogenerated carriers and AOSs.[16, 17]

Home-designed thin-layer photoelectrocatalytic flow system has exhibited great potential in organic detection and bactericidal application.[15, 17, 18] Although several works have indicated the potential of TiO_2 nanotube photoelectrode in bactericidal application, to the best of our knowledge, this is the first time to use highly ordered TiO_2 nanotube array photoelectrode combining with the thin-layer photoelectrocatalytic flow system for bactericidal application (Scheme 1).[19, 20] For this, highly ordered TiO_2 nanotube (TNT) film was successfully synthesised by a simple anodisation process. The fabricated TiO_2 nanotube array film was subsequently calcined at 450 °C for 2 h, and used as photoelectrode for photoelectrocatalytic inactivation and decomposition of *E. coli*. For comparison, TiO_2 nanoparticle (TNP) film with a similar thickness was also fabricated to evaluate its bactericidal performance.

2 Experimental section

Preparation of TNT and TNP Films

Highly ordered TNT array film was prepared by anodisation technique, as reported by our previous work.[9] Before anodisation, titanium foils (0.25 mm, 99.7%, Aldrich) were in turn washed with acetone (99.5%, Merck), isopropanol (A.R., Sigma) and deionised water (Millipore Corp., 18 MΩ·cm). The anodisation experiment was performed using a two-electrode electrochemical system at a potential of 20 V in an electrolyte solution containing 0.44% hydrofluoric acid and 12.5% acetic acid (v/v), with titanium foil as anode and platinum mesh as cathode. The as-synthesised sample was rinsed with deionised water and dried by a N_2 stream, then annealed in air at 450˚C for 2 h.

TNP film was prepared by a dip-coating method, as described in our previous work.[8] In brief, TiO_2 colloids containing *ca.* 60 g/L of TiO_2 solid with particle sizes ranging from 8 to 10 nm were prepared by hydrolysis of titanium butoxide (97%, Aldrich), and a certain amount of carbowax (30% w/w based on the solid weight of the TiO_2 colloid) was added to the colloid before use. Pretreated indium tin oxide conducting glass slides (ITO, 8

Ω/square) were then dip-coated in the colloidal solution and dried at room temperature. After dip-coating, the obtained electrodes were then calcined in a muffle furnace at 500˚C for 2 h in air.

Characterisations

The morphology and crystallinity of TNT and TNP films were characterised by scanning electron microscope (JEOL JSM-6300F, Japan) and X-ray diffraction (XRD) (Shimadzu XRD-6000 diffractometer, Japan) techniques.

Measurements

The inactivation experiments were performed in a thin-layer photoelectrocatalytic flow system with an illumination area of 4.62 cm^2 and a LED array light source, as described in our previous report.[17] The light intensity was controlled at 8.0 mW/cm^2. During bactericidal experiments, peristaltic pump was used to adjust the flowing speed of the bacteria solution and the time of inactivation and decomposition of bacteria (namely, resident time of bacteria at photoelectrode). *E. coli* cells incubated overnight at 37˚C were harvested, rinsed completely with sterilised distilled water and then diluted with 0.1 M $NaNO_3$ solution to 1.0×10^7 CFU/mL. Reaction time was controlled using a peristaltic pump by adjusting the flow rate. Before and after reaction, 1 mL of *E. coli* suspension was withdrawn, serially diluted with sterilised saline and spread on nutrient agar plates for the viability count after incubation at 37˚C for 24 h. The viability of *E. coli* was also confirmed with the fluorescent microscopic method (Live/Dead BacLight bacterial viability kit, Molecular Probes, Inc.).[21] The decomposition of *E. coli* cells was assessed with TOC-V_{CPH}-V/TOC-V_{CPN} Total Organic Carbon Analyser (Shimadzu Corporation, Japan), and the results were further confirmed by scanning electron microscope technique [17].

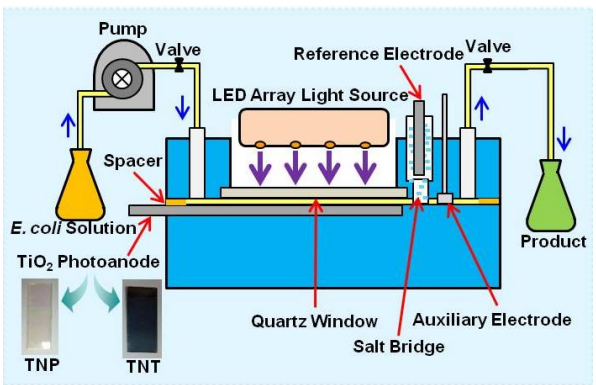

Scheme 1 Shematic diagram of thin-layer photoelectrochemical flow reactor.

3 Results and discussion

Structural characteristics

After calcination at 450˚C for 2 h, the fabricated TNT film shows uniform nanotube structures with tube diameters ranging from 60 to 100 nm and a mean length of *ca.* 486 nm (Fig. 1A and inset). Moreover, anatase phase is dominant for the TNT film after calcination, demonstrating good crystal nature of the calcined TNT film (Fig. 1B),[9] which is advantageous for improving the photocatalytic activity of the resulting photoelectrode.[11] The fabricated TiO_2 nanoparticle (TNP) film with particle sizes of 20-30 nm possesses a thickness of *ca.* 500 nm (Fig. 1C and inset). Similarly, the TNP film exhibits predominantly anatase phase after calcination at 700 ℃ (Fig. 1D).[8]

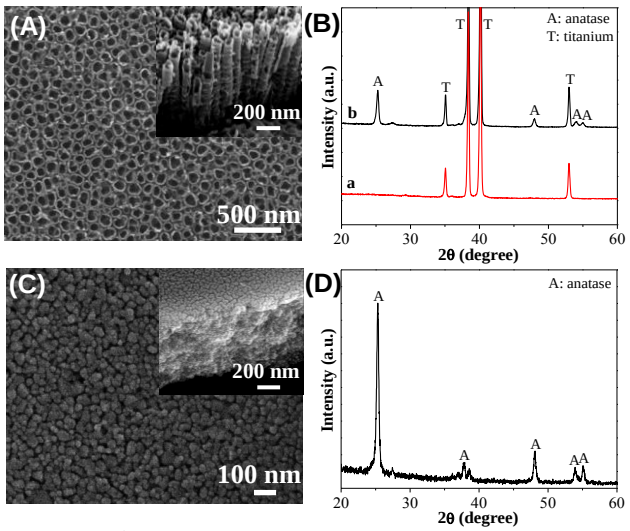

Fig. 1 (A) Surface and cross-sectional SEM images and (B) XRD patterns of TiO_2 nanotube array film; (C) Surface and cross-sectional SEM images and (D) XRD patterns of TiO_2 nanoparticle film.

Bactericidal performance

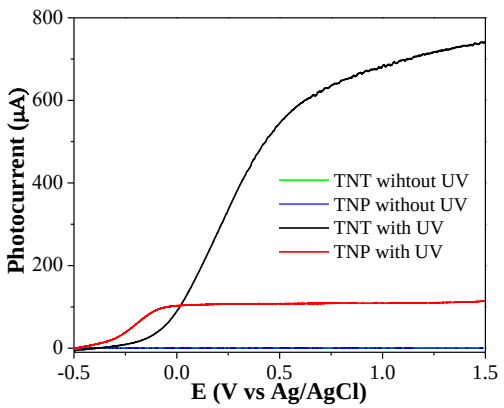

Fig. 2 Voltammograms obtained from TNT nad TNP photoelectrodes in 0.10 M $NaNO_3$ supporting electrolyte with 1.0×10^7 CFU/mL *E. coli*. UV light intensity of 8.0 mW/cm^2 and scan rate of 10.0 mV/s.

The bactericidal performance of the TNT film was investigated using *E.coli K12* as probe bacteria with an initial concentration of *ca.* 1.0×10^7 CFU/mL in a thin-layer photoelectrochemical flow reactor (Scheme 1). For comparison, inactivation experiments using a TNP film were also performed. Prior to bactericidal performance evaluation, photoelectrochemical experiments of TNT and TNP photoelectrodes were firstly conducted to choose a suitable applied potential for subsequently photoelectrocatalytic experiments. Fig. 2 shows the voltammograms of TNT and TNP photoelectrodes in 0.10 M $NaNO_3$ solution including 1.0×10^7 CFU/mL *E. coli* with or without UV light illumination. For the two photoelectrodes, only a negligible dark current can be observed. Under UV light illumination, the measured photocurrents for the two photoelectrodes initially increase linearly with the applied potential bias due to the limitation of

free photoelectron transport within the TiO_2 photocatalyst films.[8-10] The photocurrents reach a saturation state at higher potentials for the two photoelectrodes (*ca.* -0.05 V for TNP and *ca.* +0.7 V for TNT) due to the limitation of the interfacial processes at the photocatalyst/electrolyte interface.[8-10] In this work, +0.7 V of applied potential bias was choosed for the resulting inactivation experiments owing to the photocurrent reaching a saturation state at this potential for both TNT and TNP photoelectrodes.[8-10]

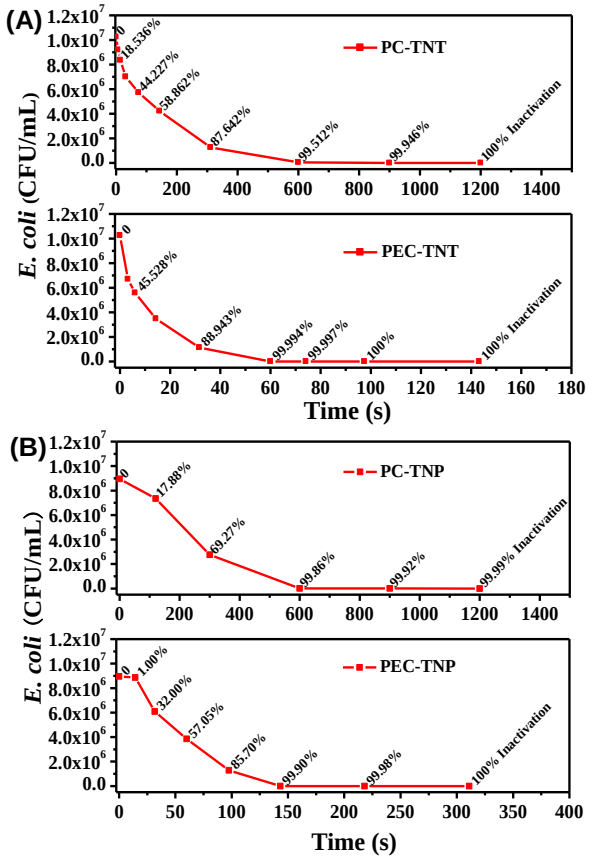

Fig. 3 Surviving *E. coli* treated by PC and PEC processes against resident time at TNT photoelectrode (A) and TNP photoelectrode (B) under UV illumination with a light intensity of 8.0 mW/cm^2 and an applied potential bias of +0.7 V.

Fig. 3A and 3B shows the inactivation results by photocatalysis (PC) and photoelectrocatalytic (PEC) using TNT and TNP photoelectrodes under UV irradiation. It is clear that the number of viable cells in all PC and PEC experiments for the two photoelectrodes decrease significantly with prolonging treated time. For TNT, it takes nearly 1200 s to achieve 100% inactivation of *E. coli* by PC, while this performance can be reached within 97 s of PEC treatment (Fig. 3A). Similarly, it requires 1200 s to obtain 99.99% inactivation by PC using TNP, however, 100% inactivation of *E. coli* can be achieved within 311 s of PEC treatment (Fig. 3B). For PC inactivation, nearly same time (*ca.* 1200 s) is needed for obtaining 100% inactivation of *E. coli* for both TNT and TNP photoelectrodes, indicating a very close PC inactivation capability of the two photocatalysts. However, the PEC inactivation efficiency of TNT is almost 2.2 times faster than that of TNP. This can be attributed to the unique nanotubular structure of TNT providing direct photoelectron transport pathway, which effectively inhibits the recombination of the photoelectron/hole pairs, dramatically increasing the PEC efficiency.[8-10] It should be noted that direct photolysis using UV light can only obtain 42.5% inactivation of *E. coli* within 1200 s, further indicating the advantages of photocatalysis and photoelectrocatalysis. For both TNT and TNP photoelectrodes, PEC process exhibits higher inactivation performance of *E. coli* than PC process, further indicating the advantage of PEC technique, namely, effectively separating the photooxidation and reduction half-reaction by applying a potential bias, thus inhibiting the recombination of photogenerated electrons and holes, and improving the photoelectrocatalytic efficiency. The PC and PEC inactivation performance of the two photoelectrodes were also confirmed using the BacLight^{TM} kit fluorescent microscopic method.[21] As shown in Fig. 4A-E, before PC and PEC treatments, all bacteria are labeled green as live *E. coli* can only accumulate Rhodamine 123. After PC and PEC treatments, *E. coli* samples become red because the dead *E. coli* bodies accumulate both Rhodamine 123 and propidium iodide under the given experimental conditions.[19] The excellent bactericidal performance of TNT photoelectrode can be due to the highly photoelectrocatalytic capability of the nanotube structure to effectively generate active oxygen species (AOSs) such as $^{\cdot}OH$, $H_2O^{\cdot}$, $O_2^{\cdot-}$, $HOO^{\cdot}$ and H_2O_2 for *E. coli* inactivation under UV irradiation.[17]

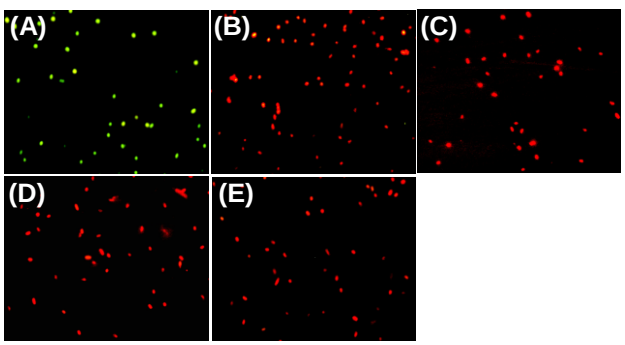

Fig. 4 Fluorescent microscopy images of *E. coli* cells under different conditions: (A) Without treatment; (B) 1200 s of PC-TNP treatment; (C) 311 s of PEC-TNP treatment; (D) 1200 s of PC-TNT treatment; (E) 97 s of PEC-TNT treatment.

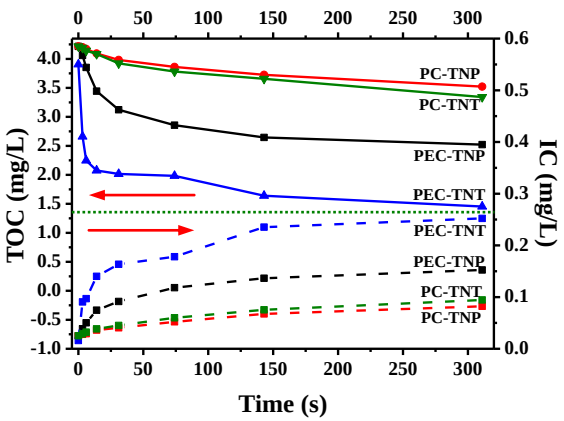

Fig. 5 TOC and IC concentration of *E. coli* solution against PC and PEC treatment time using TNT and TNP photoelectrodes.

To quantitatively study the mineralisation level of *E. coli* cells treated by PC and PEC, total organic carbon (TOC) and inorganic carbon (IC) analysis were performed for TNT and TNP. As shown in Fig. 5, a 16.4% decrease of TOC was obtained for 311 s of PC-TNP treatment, while a 20.7% decrease was achieved for 311 s of PC-TNT treatment. However, the TNT exhibits a 62.8% decrease of TOC after 311 s of PEC treatment, which is much higher than that using TNP (40.2%). The above results were further confirmed by IC analysis, as it can be observed that in all cases, IC amount increases slightly with the decrease of TOC, which is in consistence with the TOC data. It is noticeable that the increase of IC is not equal to the decrease amount of TOC, which can be attributed to the low solubility of CO_2 evolved from the mineralisation of intracellular constituents and framework of *E. coli*, indicating that the biological carbon contents were mineralised to the ground.[22] The above results further support the excellent PEC activity of TNT for bactericidal application compared to TNP.

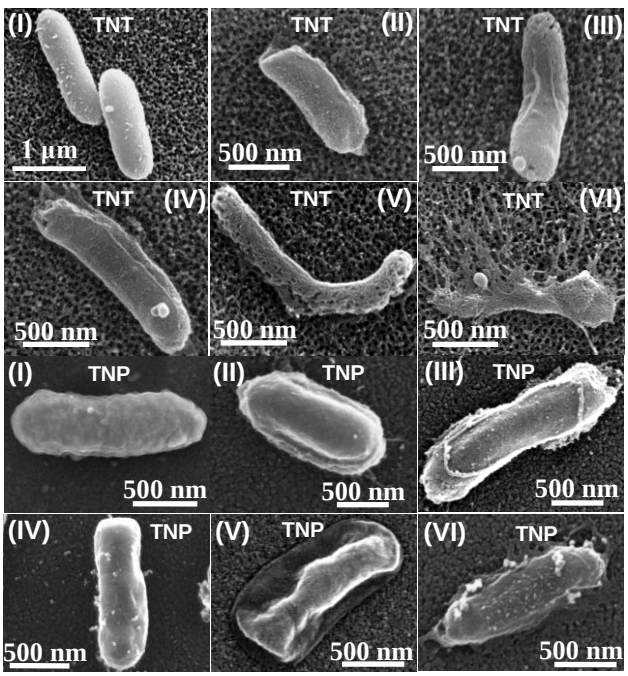

Fig. 6 SEM images of *E. coli* cells attached onto the TNT and TNP films with different treatment conditions. TNT(I) and TNP(I): Without treatment; TNT(II) and TNP(II): 600 s of PC treatment; TNT(III) and TNP(III): 900 s of PC treatment; TNT(IV) and TNP(IV): 60 s of PEC treatment; TNT(V) and TNP(V): 150 s of PEC treatment; TNT(VI) and TNP(VI): 300 s of PEC treatment.

Electron microscopy technique was employed to further examine the decomposition level of *E. coli* cell attached onto TNT and TNP films after PC and PEC treatments. Fig. 6 shows the SEM images of *E. coli* cells on the TNT and TNP films before and after PC and PEC treatments. As shown, the untreated cells present well-preserved cell walls (TNT(I) and TNP(I)), suggesting that the bacteria are active and healthy. No matter TNT or TNP with PC treatment, *E. coli* cells display a slight change in shape after short treatment time (*e.g.*, 600 s, TNT(II) and TNP(II)). With prolonging PC treatment time to 900 s, severe damages can be observed on the cell wall (TNT(III) and TNP(III)). The cell damage can be due to the AOSs' role, such as ·OH, HOO· and H_2O_2.[14, 17] With PEC treatment, the TNT exhibits significantly improved decomposition capability (TNT(IV, V, VI) in comparison with the TNP (TNP(IV, V, VI)). With 300 s of PEC treatment, the *E. coli* cell is almost decomposed completely using TNT (TNT(VI)), which is apparently better than using TNP (TNP(VI)), further indicating the superior PEC decomposition capability of *E. coli* cell for TNT. The above results combining with TOC/IC data provide a direct evidence to confirm the PEC treatment able to facilitate the decomposition of *E. coli* compared to the PC treatment for both electrodes. This can be attributed to the PEC approach effectively decreasing the recombination of photoelectrons and holes, thus improving the lifetime of the photogenerated carriers and AOSs and the photoelectrocatalytic performance.[17] Moreover, the TNT possesses much higher capability to rapidly decompose *E. coli* cells than the TNP, owing to its unique one-dimensional nanotubular structures with the superior electron transport characteristics.[9] The stability of the TiO_2 nanotube film for photoelectrocatalytic inactivation of *E. coli* after reuse was evaluated by a 10 successive inactivation experiments. As shown in Fig. 7, no obvious bactericidal performance change was observed, demonstrating a superior stability of the TiO_2 nanotube photoelectrode.

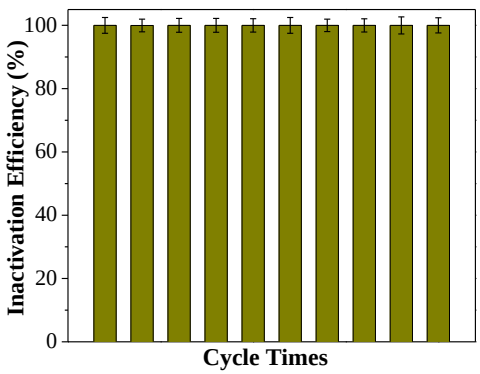

Fig. 7 Bactericidal stability of anatase TiO_2 nanotube film by photoelectrocatalytic technique. The concentration of *E.* coli of 1×10^7 CFU/mL, light intensity of 8.0 mW/cm^2, an applied potential bias of +0.7 V and the resident time of 60 s.

4 Conclusions

In conclusion, highly ordered TNT film was prepared, and used as photoelectrode to evaluate the bactericidal performance in a thin-layer photoelectrochemical flow reactor. Compared to TNP, the TNT exhibited superiorly photoelectrocatalytic performance for instant inactivation and rapid decomposition of *E. coli*. This work demonstrates the possibility of using high efficiency TiO_2 nanotube photoelectrode combing with thin-layer photoelectrochemical flow reactor for effective removal of waterborne pathogens.

This work was financially supported by Australian Research Council (ARC) Discovery Project.

Notes and references

[a] *Centre for Clean Environment and Energy, Griffith University, Gold Coast Campus, Queensland 4222, Australia. Fax: +61 7 55528067; Tel: +61 7 55528456; E-mail: haimin.zhang@griffith.edu.au*
[b] *Department of Environmental Engineering, Beijing Institute of Petrochemical Technology, 19 Qingyuan North Road, Daxing District, Beijing 102617, China. E-mail: hanyanhe@126.com*
[c] *State Key Laboratory of Organic Geochemistry, Guangzhou Institute of Geochemistry, Chinese Academy of Sciences, Guangzhou 510640, China.*

1. S. Zhang, J. Qiu, J. Han, H. Zhang, P. Liu, S. Zhang, F. Peng and H. Zhao, *Electrochem. Commun.*, 2011, **13**, 1151-1154.
2. Y.-Y. Song, F. Schmidt-Stein, S. Bauer and P. Schmuki, *J. Am. Chem. Soc.*, 2009, **131**, 4230-4232.
3. Y.-Y. Song and P. Schmuki, *Electrochem. Commun.*, 2010, **12**, 579-582.
4. P. A. Mandelbaum, A. E. Regazzoni, M. A. Blesa and S. A. Bilmes, *J. Phys. Chem. B*, 1999, **103**, 5505-5511.
5. H. Zhang, X. Liu, Y. Wang, P. Liu, W. Cai, G. Zhu, H. Yang and H. Zhao, *J. Mater. Chem. A*, 2013, **1**, 2646-2652.
6. K. Zhu, N. R. Neale, A. Miedaner and A. J. Frank, *Nano Lett.*, 2006, **7**, 69-74.
7. W. Hu, Y. Zhao, Z. Liu and Y. Zhu, *Nanotechnol.*, 2007, **18**, 095605/095601-095605/095605.
8. D. Jiang, H. Zhao, S. Zhang and R. John, *J. Phys. Chem. B*, 2003, **107**, 12774-12780.
9. H. Zhang, H. Zhao, S. Zhang and X. Quan, *ChemPhysChem*, 2008, **9**, 117-123.
10. H. Zhang, X. Liu, Y. Li, Q. Sun, Y. Wang, B. J. Wood, P. Liu, D. Yang and H. Zhao, *J. Mater. Chem.*, 2012, **22**, 2465-2472.
11. M. Tian, S. S. Thind, S. Chen, N. Matyasovzsky and A. Chen, *Electrochem. Commun.*, 2011, **13**, 1186-1189.
12. T. Matsunaga, R. Tomoda, T. Nakajima and H. Wake, *FEMS Microbiol. Lett.*, 1985, **29**, 211-214.
13. T. Saito, T. Iwase, J. Horie and T. Morioka, *J. Photochem. Photobiol. B*, 1992, **14**, 369-379.
14. M. Cho, H. Chung, W. Choi and J. Yoon, *Water Res.*, 2004, **38**, 1069-1077.
15. S. Zhang, D. Jiang and H. Zhao, *Environ. Sci. Technol.*, 2006, **40**, 2363-2368.
16. S. H. Kang, S.-H. Choi, M.-S. Kang, J.-Y. Kim, H.-S. Kim, T. Hyeon and Y.-E. Sung, *Adv. Mater.*, 2008, **20**, 54-58.
17. G. Li, X. Liu, H. Zhang, T. An, S. Zhang, A. R. Carroll and H. Zhao, *J. Catal.*, 2011, **277**, 88-94.
18. G. Li, X. Liu, H. Zhang, P.-K. Wong, T. An and H. Zhao, *Appl. Catal. B*, 2013, **140–141**, 225-232.
19. M. F. Brugnera, M. Miyata, G. J. Zocolo, C. Q. F. Leite and M. V. B. Zanoni, *Electrochim. Acta*, 2012, **85**, 33-41.
20. N. Baram, D. Starosvetsky, J. Starosvetsky, M. Epshtein, R. Armon and Y. Ein-Eli, *Electrochim. Acta*, 2009, **54**, 3381-3386.
21. Y. Liu, X. Wang, F. Yang and X. Yang, *Micropor. Mesopor. Mater.*, 2008, **114**, 431-439.
22. D. D. Sun, J. H. Tay and K. M. Tan, *Water Res.*, 2003, **37**, 3452-3462.